Title: **Spatial variation in introgression along a toad hybrid zone in France**

Running title: Variation in introgression along a toad hybrid zone

Authors: I. van Riemsdijk[1,2*], J.W. Arntzen[1], G. Bucciarelli[3,4], E. McCartney-Melstad[3,4], M. Rafajlović[5], P.A. Scott[3], E. Toffelmier[3,4], H. B. Shaffer[3,4], B. Wielstra[1,2]

Affiliations:
[1]Naturalis Biodiversity Centre, Leiden, the Netherlands
[2]Institute of Biology Leiden, Leiden University, Leiden, the Netherlands
[3]Department of Ecology and Evolutionary Biology, UCLA, Los Angeles, California
[4]La Kretz Center for California Conservation Science, Institute of the Environment and Sustainability, UCLA, Los Angeles, California
[5]Department of Marine Sciences, University of Gothenburg, Gothenburg, Sweden

*Correspondence: Isolde van Riemsdijk, isolde.vanriemsdijk@naturalis.nl

Author contributions: IvR, JWA, BS, and BW designed the study. IvR and JWA collected samples. IvR performed the laboratory work and data assembly with contributions from GB, EMM, PS, ET and MR. IvR analysed the data and wrote the manuscript with input from all authors.

Acknowledgements: We thank Frido Welker, Tara Luckau, Roger K. Butlin, the members of the Butlin laboratory at the University of Sheffield, and the Allentoft laboratory at the Natural History Museum in Copenhagen for support and discussion. The PhD position of IvR is supported by the 'Nederlandse Organisatie voor Wetenschappelijk Onderzoek' (NWO Open Programme 824.14.014). This project has received funding from the European Union's Horizon 2020 research and innovation programme under the Marie Skłodowska-Curie grant agreement No. 655487. Part of this project was carried out at the Shaffer laboratory in Los Angeles, at the University of California. This study trip has been sponsored by the Leiden University Fund / Swaantje Mondt Fonds (D7102).

Data Accessibility Statement: In- and output of analyses, and custom R scripts will be available at Dryad. Raw sequencing data will be available at GenBank.

Spatial variation in introgression along a toad hybrid zone in France

Abstract

The barrier effect is a restriction of gene flow between diverged populations by barrier genes. Asymmetric introgression can point to selection, hybrid zone movement, asymmetric reproductive isolation, or a combination of these. Restriction of gene flow and asymmetric introgression over multiple transects point towards influence of intrinsic (genetic) rather than extrinsic (climate) factors. The 900 km long hybrid zone between *Bufo bufo* and *B. spinosus* toads permits the study two widely separated transects (northwest and southeast France) using restriction-site associated DNA (RAD) sequencing data. Genomic and geographic clines were used to identify outlier markers with restricted or elevated introgression. Twenty-six barrier markers are shared between transects, but the number of barrier markers is twice as high in the southeast transect. In the northwest transect a high amount of introgression from *B. spinosus* into *B. bufo* is most consistent with asymmetric reproductive isolation. In the southeast transect, introgression is symmetric and consistent with a stable hybrid zone. Differences between transects may be related to genetic sub-structuring within *B. bufo*, suggesting that reproductive isolation between the two species has a common genetic origin, but a longer period of secondary contact in southeast France appears to result in a stronger barrier effect (reinforcement) than in the northwest.

Keywords: Asymmetric introgression; barrier genes; *Bufo bufo*; *Bufo spinosus*; replicate transects; reinforcement.

Introduction

Hybrid zones provide an opportunity to study both the processes involved in, and the outcomes of, speciation (Hewitt, 1988). Barrier genes, defined as genomic regions that restrict gene flow

(or introgression) between hybridizing populations, play a key role in speciation (Ravinet et al., 2017). Barrier genes can comprise genes involved in divergent ecological selection, mate choice, and genetic incompatibilities (Ravinet et al., 2017). Barrier genes are responsible for creating genomic heterogeneity in interspecific divergence, with relatively strong differentiation of the barrier genes themselves as well as the genomic regions surrounding them, and prohibit homogenization of the parental populations (Abbott et al., 2013; Barton, 2013; Ravinet et al., 2017). The barrier effect is a reduction of effective migration rate of genetic material between populations, relative to the dispersal of the individuals carrying those genes (Ravinet et al., 2017). Barrier genes and their linked loci (together referred to as 'barrier markers' here) are expected to show relatively steep transitions at species boundaries (Gompert, Parchman, & Buerkle, 2012; Butlin & Smadja, 2018). This barrier effect is reinforced when the gene frequency clines of multiple barrier genes become geographically coincident in a hybrid zone, a phenomenon referred to as cline coupling (Butlin & Smadja, 2018). When the same markers show such steep and co-distributed transitions along multiple geographically distant transects across a hybrid zone, it is most likely that the two hybridizing species evolved barrier effect across their entire species' range (Teeter et al., 2009; Larson, Andrés, Bogdanowicz, & Harrison, 2013; Harrison & Larson, 2014; Larson, White, Ross, & Harrison, 2014).

Within a transect, patterns of introgression can be indicative of different types of selection. Asymmetric introgression in hybrid zones, where gene flow is more pronounced in one direction than in the other, can be caused by hybrid zone movement, positive selection, asymmetric reproductive isolation, or both. Hybrid zone movement occurs when, for example, one species outcompetes the other, and can cause elevated introgression of many neutral markers in the wake of the movement (Gay, Crochet, Bell, & Lenormand, 2008; Excoffier, Foll, & Petit, 2009; Wielstra, Burke, Butlin, & Arntzen, 2017; Wielstra, Burke, Butlin, Avcı,

et al., 2017; Wielstra, 2019). On the other hand, adaptive introgression would typically concern only one or a few markers (Barton & Hewitt, 1985; Barton, 2001). Asymmetric pre- or postzygotic isolation involves the successful reproduction of only certain combinations of individuals (e.g. hybrids can only backcross with individuals of one of the species involved), and most of the introgression takes place on the side of the hybrid zone where interspecific reproduction is the most successful (Haldane, 1922; Hewitt, 1975; Barton, 2001; Devitt, Baird, & Moritz, 2011). As hybrid populations receive more genes from the side of the hybrid zone where reproduction is most successful, asymmetric reproductive isolation can have the effect of a competitive advantage, and thus result in hybrid zone movement (Buggs, 2007).

We study a ca. 900 km long hybrid zone between the common toad, *Bufo bufo* (Linnaeus, 1758) and the spined toad, *B. spinosus* Daudin, 1803, running diagonally across France from the Atlantic coast to the Mediterranean coast in the very northwest of Italy (Fig. 1; Arntzen et al., 2018). Given the low dispersal of both species, the length of the hybrid zone provides an opportunity to test the consistency of patterns of restricted gene flow and elevated directional gene flow in independent transects. We study two transects at opposite ends of the hybrid zone, one in the northwest and one in the southeast (Fig. 1). Previous studies on the individual transects suggested that weak asymmetric introgression may be occurring in both sections (Arntzen, de Vries, Canestrelli, & Martínez-Solano, 2017; van Riemsdijk, Butlin, Wielstra, & Arntzen, 2018). Here we consult ~1200 nuclear markers, two to three orders of magnitude than used in previous studies, to assess genome wide patterns on introgression in this hybrid zone. Assuming that reproductive isolation is consistent throughout the hybrid zone, the same barrier genes should be consistently reducing gene flow between the two species in both transects. If patterns of (asymmetric) introgression are similar, this would indicate an intrinsic (e.g. genetic) cause, whereas if patterns are different, they may indicate local (transect-specific) intrinsic or extrinsic (environmental) factors.

Material and Methods

3RAD sequencing

DNA extracts of 387 individual toads were reused from previous research (Arntzen et al., 2016, 2017, 2018, in prep.). We included five reference sample sites each of presumably pure *B. bufo* and *B. spinosus*, 11 sample sites in transect one in northwest France, and 12 sample sites in transect two in southwest France (Table S.1.; Fig. 1). For three presumably pure individuals of each species, libraries were prepared in triplicate (6 individuals x 3 = 18) to assess genotyping error rate after assembly (which was estimated to be 0.5%; Appendix 1). The 3RAD method (Graham et al., 2015; Glenn et al., 2016; Hoffberg et al., 2016; Bayona-Vásquez et al., 2019) was used to obtain reduced representation genomic libraries. Two restriction enzymes (CLA-*I* and Sbf-*I*) were used to cut 50 ng of genomic DNA from each sample, while a third enzyme (MSP-*I*) was added to cleave and eliminate phosphorylated adapter-adapter dimers. Internal barcodes were ligated to the resulting sticky ends and external Illumina iTru5 and iTru7 primers, differing by ≥ 3 bp, were added to the internal barcodes via an indexing PCR reaction (Glenn et al., 2016; Hoffberg et al., 2016; Bayona-Vásquez et al., 2019).

To 5 µL of DNA extract, 1.5 µL of Cutsmart buffer (New England Biolabs, Ipswich, MA; NEB), 0.5 µL of each digestion enzyme, and 5 µL of purified water were added. Digestion took place for 3h at 37 °C. For internal primer ligation, 1 µL of 100 units/uL DNA ligase, 0.5 µL of ligase buffer (NEB), 1.5 µL of rATP and 2 µL of purified water were added and the samples were heated for two cycles of 20 min on 22 °C and 10 min on 37 °C, ending with 20 min at 80 °C. The ligated DNA product was purified with 2X SPRI beads (GE Healthcare Bio-Sciences, Marlborough, MA; see Glenn *et al*., 2016 and Appendix 2 for details). The external dual index primers were added through PCR by adding 15 µL of Kapa HiFi HS RM (Kapa Biosystems, Wilmington, MA), and 2.5 µl of each iTru5 and iTru7 primer to 5 µl of purified DNA from the

previous step, with a PCR programme of 95 °C for 2 min, and 20 cycles of 98 °C for 20 sec, 60 °C for 15 sec, 72 °C for 30 sec, ending with 72 °C for 5 min, and held at 15 °C.

After a second purification step the DNA concentrations of seven libraries contained less than the required concentration for equimolar pooling, even after repeating the library preparation twice, thus the total volume of the library was included in the pool. All other libraries were combined to achieve equimolar concentrations in the final pool. The fragments in the pooled library were size selected for a range of 340-440 bp using a Pippin Prep (Sage Science Inc. Beverly, MA), quantified using intercalating dye on a Victor multilabel plate reader, and were sequenced on two lanes of an Illumina HiSeq 4000 PE100 at the Vincent J. Coates Genomics Sequencing Laboratory in Berkeley, CA, USA.

Data clean-up and assembly

The average read count per sample was ~1.5 million reads (maximum 4.2 million reads, Table S.2). Twelve samples had low raw read quantities (near or below 0.5 million reads), including the seven samples with low DNA concentration, and were excluded (file size <10.000 kb). Cutadapt v.1.14 (Martin, 2011) was used in three steps to remove 5' and 3' primers for each internal barcode combination, remove the Illumina standard adapter, and carry out a read quality control. Subsequently, ipyrad v.0.7.3 (Eaton, 2014) was used to assemble the reads. Settings were: minimum read depth of six, maximum of eight heterozygous bases allowed per consensus sequence, and heterozygous sites allowed across a maximum of 50% of the samples (details in the supplements). We assembled three data sets in which the minimum number of individuals that must have data for each locus to be retained was 194 (50% of the samples), 291 (75%) and 349 (95%) of the 387 total samples to generate matrixes with different levels of missing data for downstream analyses. After assembly, two additional individuals were

157 excluded because of low read counts. The 50% dataset contained 4,863 markers and 39,750
158 SNPs.
159
160 **Population structure**
161 Using a single randomly selected SNP per RAD fragment from the 50% dataset, we first ran a
162 principal component analysis (PCA) to visualize genomic variation across both transects. We
163 used the package 'adegenet' v.2.1.1 in R (Jombart, 2008; Jombart & Ahmed, 2011), and based
164 the PCA on allele frequencies, replacing missing data with the mean of the total dataset. We
165 further quantified population structure with Structure v.2.3.4 (Pritchard, Stephens, & Donnelly,
166 2000) with the same dataset, for each transect separately. Preliminary results showed that using
167 a dataset with loci for which at least 75% or 90% of individuals have data, returned similar
168 results as using the dataset for which at least 50% of individuals have data. Therefore, in
169 downstream analyses we used the 50% dataset, or subsets of the 50% dataset. We ran Structure
170 with ten replicates each of two to ten genetic clusters (*K*) with a burn in of 10,000 and a chain
171 length of 25,000 under the admixture model using StrAuto (Chhatre & Emerson, 2017).
172 Convergence of the results was checked by investigating log likelihood and admixture
173 proportion stability (Benestan et al., 2016). The results were summarized with CLUMPAK
174 (Kopelman, Mayzel, Jakobsson, Rosenberg, & Mayrose, 2015). The best value of *K* was
175 determined with the Evanno method (Evanno, Regnaut, & Goudet, 2005). Structure results
176 were visualised using the R package POPHELPER (Francis, 2017).
177
178 **Diagnostic SNP selection**
179 Diagnostic SNPs were determined based on the genotypes of the 37 *B. bufo* and 20 *B. spinosus*
180 individuals from the reference sample sites (Fig. 1; Table S.1, custom R script). We selected
181 all SNPs for which a maximum of 70% of the data was missing in each species and selected

all bi-allelic SNPs that were fixed for alternative homozygous variants in the set of reference samples of each species. We selected one random diagnostic SNP per fragment, resulting in 1,189 diagnostic SNPs.

Hardy-Weinberg equilibrium

We tested for signals of non-random mating success for each sample site in the dataset with diagnostic SNPs by calculating heterozygote excess and deficit from Hardy-Weinberg equilibrium with the R package 'genepop' based on the program GENEPOP v.1.0.5 (Rousset, 2008). Instead of the conservative Bonferroni correction, which accounts for the number of tests performed in total, independence of tests was accounted for within markers (P_c for N=1,189; Rice 1989; Narum 2006). Many markers with a significance level uncorrected for repeated testing ($P < 0.05$) in the hybrid zone populations for both heterozygote excess and absence were present, but only 14 markers had a significant heterozygote deficit after correction (Table S.3). These markers were excluded in the HZAR geographic cline fitting analysis and admixture linkage disequilibrium calculations (see below).

Bayesian genomic cline outlier detection

To study genome-wide variation of introgression among admixed individuals we used the Bayesian genomic cline model as implemented in the software BGC (Gompert & Buerkle, 2011, 2012; Gompert et al., 2012). The Bayesian genomic cline model is based on the probability that an individual with a certain hybrid index (HI) inherited a gene variant at a given locus from one species (φ; in this case *B. bufo*) or the other ($1 - \varphi$; *B. spinosus*). The probability of *B. bufo* ancestry relative to expected (represented by the HI) is described by cline parameter α. A positive α indicates an increase in the *B. bufo* ancestry probability and a negative α indicates a decrease. The cline parameter β measures the genomic cline rate based on ancestry

for each locus. A positive β indicates an increased transition rate from a low to high probability of *B. bufo* ancestry as a function of the HI, which implies there are less heterozygotes for the marker than expected based on the HI, whereas a negative β indicates a decrease in the transition rate, which implies there are more heterozygotes than expected based on the HI (Gompert & Buerkle, 2011; Parchman et al., 2013). When more markers are an outlier for α in one direction than the other, this points to genome wide asymmetric introgression. When a marker is a negative outlier for cline parameter β, it is a candidate for a barrier marker, especially when the geographic cline is narrow and located in the centre of the hybrid zone.

The input files for parental genotypes included only individuals from the reference sample sites, and the input file for admixed genotypes included individuals with an average admixture proportion (Structure Q score) between 0.05 and 0.95, treated as a single population (Fig. S.1). A single MCMC chain was run for 75,000 steps and samples were taken from the posterior distribution every 5th step, following a burn-in of 25,000 steps. Convergence was assessed (Fig. S.2), and we tested for outlier loci using 'estpost' to summarise parameter posterior distributions (Gompert & Buerkle, 2011). Outlier loci were established based on 99.9% confidence intervals of parameters.

Geographic cline analysis

Classic geographic equilibrium cline models were fitted using the R package 'HZAR' (Derryberry, Derryberry, Maley, & Brumfield, 2014) for all diagnostic SNPs. For transect one, sample sites 6 and 16, which are distant from the main axis of the transect, were removed from the dataset. To determine distance between the sample sites, a custom R script was used, and the directions of the transect axes were the same as in previous publications (Arntzen et al., 2016, 2017). The shapes and positions of many clines can be summarised in the expected cline, which can be represented by the HI (Polechová & Barton, 2011; Fitzpatrick, 2012). We thus

also fitted clines for the HI of all non-outlier markers as determined by BGC, as well as the HI of all heterozygote deficiency outliers ($\beta > 0$), to be able to compare the shape and positions of these categories in a geographical setting. The heterozygote deficiency outliers are expected to be geographically steep clines. Thirty maximum likelihood estimation searches were performed with random starting parameters, followed by a trace analysis of 60,000 generations on all models with a delta Akaike Information Criterion corrected for small-sample-size (dAICc) < 10. Fifteen model variants were based on all possible combinations of trait intervals (allele frequency at the ends of the transects; three types) and tail shape (five types). Even though markers were restricted to be diagnostic, cline shapes sometimes were better described by clines with allele frequencies at the end of the cline different from zero or one. Convergence was visually assessed in trace plots (see supplemental material). To provide a measure of cline symmetry, we used a custom R script to estimate the area underneath the cline tail towards the left (Q_{left}) and the right (Q_{right}) of the hybrid zone centre, up to the point where the HI reached a value of 0.05 or 0.95 (Fig. S.3, supplements).

Admixture linkage disequilibrium and effective selection

To assess the most recent inflow of parental genotypes, linkage disequilibrium can be used. The first generation offspring of two diverged species will be heterozygous for all fixed differences, resulting in complete admixture linkage disequilibrium (D'), rather than the usual linkage disequilibrium resulting from selection, assortment, mutation, or drift (Barton & Gale, 1993; Baird, 2015). Recombination during reproduction breaks down D', whereas migration of parental (pure) individuals increases D' (Barton & Gale, 1993). When gene flow into the hybrid zone is symmetric, the peak of D' in the hybrid zone centre follows a Gaussian curve (Gay et al., 2008). Under hybrid zone movement, the peak is predicted to shift ahead of the movement to the side of the hybrid zone, opposite to the tail of neutral introgression where

recombination has broken down the peak already (Gay et al., 2008; Wang et al., 2011). The peak is expected to be more coincident with the tail of introgression in a case of asymmetric reproductive isolation (Devitt et al., 2011). The position of the peak of D' thus may be used to support the underlying process of asymmetric introgression.

Average effective selection on a locus (s*) is the selection pressure on a locus at the zone centre due to direct selection and association with other loci. Admixture linkage disequilibrium (*D*') based on the variance in hybrid index, which in turn allows the calculation of lifetime dispersal distance weighted for pre- and post- metamorphosis (σ), and s* following Barton & Gale (1993), were calculated using scripts from van Riemsdijk et al. (2019). The data contained only markers in Hardy-Weinberg equilibrium and markers not indicated as outliers in BGC (832 and 652 loci) for each transect, because these markers represent the presumably neutral portion of the genome (Table 1). We repeated the analysis using only the markers that were heterozygote deficiency outliers ($\beta > 0$; 56 and 121 loci) to represent the portion of the genome that experiences the highest barrier effect. Fixed parameters were: a recombination rate of 0.4997, calculated following formula (6) from Macholán et al. (2007), using the number of chiasmata per bivalent for *B. bufo* (1.95; Wickbom, 1945) and the number of chromosomes for *B. bufo* (N = 22), a generation time of 2.5 years for *Bufo* at the latitude of the hybrid zone (mean of 3 years in females and 2 years in males; Hemelaar, 1988) and initial secondary contact 8,000 years ago following Arntzen et al. (2016). The width of the hybrid zone was derived from a general sigmoid cline model following HZAR (Derryberry et al., 2014), fitted to the HI. Mean and 95% confidence interval (CI) were based on 1,000 bootstrap replicates of the original genotype dataset (with replacement, maintaining original sample size within sites). Following Gay et al. (2008), we fitted a Gaussian curve through the estimates of *D'* and 95% confidence intervals (CI) for the calculated parameters were derived from the bootstrap data.

Results

The first axis (PC1, 26.8%) of the PCA appears to reflect the genetic difference between pure *B. bufo* in the north (right) and pure *B. spinosus* in the south (left), with hybrids in the middle (Fig. S.4). The second axis (PC2, 2.8%) separates the two transects. In Structure, the preferred number of genetic clusters for transect one was K=3, and for transect two K=2 (Fig. S.1). In both transects, the plot for two genetic clusters reflects differentiation between the two species, with hybrids smoothly transitioning between the two, while the three-cluster model places hybrids in a group of their own.

The dataset in the BGC analysis covers the different hybrid index (HI) bins well (Fig. S.5). Transect one has significantly more markers with a reduced probability of *B. bufo* ancestry ($\alpha < 0$, n = 151) than markers with an increased probability ($\alpha > 0$, n = 110, χ^2 test $P = 0.0112$; Table 1), relative to the hybrid index. Transect two has a nearly equal number of markers with an increased or decreased probability of *B. bufo* ancestry ($\alpha > 0$, n = 174; $\alpha < 0$, n = 185, χ^2 test $P = 0.5615$). The number of markers with an outlier β in transect one (heterozygote deficiency $\beta > 0$, n = 56 and heterozygote excess $\beta < 0$, n = 42) is about half the number detected in transect two ($\beta > 0$, n= 123, and $\beta < 0$, n = 105). Of the RAD markers which are positive or negative outliers for α or β, 22-61% are also outliers in transect two (last column Table 1). Such overlap is unlikely if the two transects were completely evolutionarily independent (Table 1). For example, the chance of the same 26 markers to act as barrier markers in both transects by chance is close to zero (last row Table 1).

We verified that outlier markers for α or β in the BGC analysis are correlated to outlier behaviour in the shape and position of their geographic cline, by plotting significant outliers for the parameters α and β from BGC to the geographic cline parameters centre and width determined with HZAR (Fig S.6). When a marker is an outlier for α, it would be expected that the cline is shifted (centre) or has a different shape (e.g. width), or both, compared to the

genomic average (e.g. represented by the HI cline). When a marker is an outlier for heterozygote deficiency ($\beta > 0$) it should also show a steep and geographic cline coincident with the HI cline (green clines, Fig. 2, Fig. S.6). We refer to such markers as 'barrier markers'. Markers that are not outliers within a transect are referred to as 'neutral markers'.

The HI cline based on neutral markers in transect one (northwest France) shows a high level of asymmetric introgression from *B. spinosus* into *B. bufo* by a fitted cline shape with a tail ($Q_{left} = 15.0$, $Q_{right} = 8.8$), whereas transect two (southeast France) shows a pattern of symmetric introgression by a cline shape without tails ($Q_{left} = 11.0$, $Q_{right} = 11.0$; Fig. 2, Table S.4, Fig. S.8). The cline widths for neutral markers in both transects are similar (47 km and 49 km), and the cline shape in the centre is generally steep (Fig. 3). The HI clines for barrier markers are symmetrical in both transects (Table S.4).

In both transects, the admixture linkage disequilibrium (D') for neutral markers shows a peak in the centre of the hybrid zone, although the amplitude of the peak in transect one is one fifth of the peak in transect two (Fig. 2). As barrier markers are less likely to flow away from the hybrid zone centre, the peak of D' for barrier markers may be more sensitive to shifts of the hybrid zone centre. In transect one, barrier markers showed a peak with higher D' on the *B. bufo* side of the hybrid zone, but displacement of the Gaussian curve was not significant; as the AIC was nearly equal when constraining the peak of D' to the cline centre (435 km) as when the peak was fitted unconstrained (resulting in a peak at 423 km). In transect two, barrier markers showed a peak of D' in the centre of the hybrid zone.

The lower peak of D' in transect one corresponds to a lower number of steep clines observed, and underlies the lower estimates of effective selection against hybrids (s*) and lifetime dispersal compared to transect two. For transect one s* is 0.0022 (95% CI 0.0012-0.0034) whereas it is about an order of magnitude greater for transect two, where s* is 0.0195 (95% CI 0.0143-0.0252; Table S.5). Notably, the confidence intervals do not overlap. The s*

based on barrier markers for transect one is 0.0101 (95% CI 0.0054-0.0152) and for transect two 0.0344 (95% CI 0.0220-0.0470). We estimated the lifetime dispersal distance based on neutral markers for transect one and two at 1.8 (95% CI 1.3-2.2) and 4.0 (95% CI 3.4-4.5) km per generation, respectively.

Discussion

The opportunities and limitations of genes to flow between hybridizing populations provide insight into the speciation process. Consistency of barrier genes (or barrier markers in tight linkage with them) over multiple transects suggests that the two hybridizing species evolved a range wide barrier effect between them (Teeter et al., 2009; Larson, Andrés, et al., 2013; Harrison & Larson, 2014; Larson et al., 2014). When introgression shows asymmetry over multiple transects, an intrinsic factor (e.g. genetically determined) is more likely the cause of the asymmetry than an extrinsic environmental factor (e.g. climate) that may vary across space. In this context we tested the consistency of barrier markers and introgression for two transects on opposite sides of the *Bufo* hybrid zone.

A barrier to gene flow in Bufo *transects*

The data presented covers only a small proportion of the genome, and outlier markers likely reflect regions in linkage with the actual barrier genes, therefore we use the term 'barrier markers'. The number of barrier markers in transect one is approximately half that of transect two, and selection against hybrids is significantly lower in transect one (northwest France), with 56 barrier markers, than in transect two (southeast France), with 123 barrier markers (Table 1, Table S.5). However, the two transects also share 26 barrier markers, which is unlikely to be the result of chance. The barrier markers shared across both transects may be clustered in a few low-recombination regions.

During postglacial expansion, secondary contact between *B. bufo* and *B. spinosus* was first established in the southeast of France and at a later point in the northwest (Arntzen et al., 2017). As a consequence, cline coupling may have progressed differently towards reproductive isolation (reinforcement) after secondary contact (Harrison & Larson, 2016; Butlin & Smadja, 2018; Dagilis, Kirkpatrick, & Bolnick, 2019). The higher the number of barrier genes restricting gene flow, the higher the overall effective selection against hybrids (Barton, 1983; Barton & Gale, 1993; Bierne, Welch, Loire, Bonhomme, & David, 2011; Vines et al., 2016). The number of barrier genes and the strength of effective selection against hybrids, which can only be directly observed in a hybrid zone, can thus be used as an indication of the progress of speciation. On the other hand, species divergence with gene flow is predicted to result in more clustering of divergent loci, of which a subset will be barrier genes, than under species divergence without gene flow (Noor, Grams, Bertucci, & Reiland, 2001; Rieseberg, 2001; Emelianov, Marec, & Mallet, 2004; Nosil, Funk, & Ortiz-Barrientos, 2009; Yeaman & Whitlock, 2011; Harrison & Larson, 2016; Rafajlović, Emanuelsson, Johannesson, Butlin, & Mehlig, 2016; Schumer et al., 2018). Whether the higher number of barrier markers observed in the southeast of France is due to the presence of a higher number of barrier genes, or lower recombination rate surrounding barrier genes is not possible to determine with the current dataset. A linkage map would provide the evidence to distinguish between (physical) linkage of barrier genes, or the presence of a higher number of barrier genes.

High similarity of restricted gene flow in multiple transects pointed to intrinsic similarities of a barrier effect in the sunflower (*Helianthus*) hybrid zone, one of the first hybrid zones studied with multiple transects, with gene flow restricted by genomic regions linked to pollen sterility and chromosomal rearrangements (Rieseberg, Whitton, & Gardner, 1999; Buerkle & Rieseberg, 2001). Under laboratory conditions the barrier genes were also found to restrict gene flow, which excluded the possibility of the involvement of external factors (Buerkle &

Rieseberg, 2001). In field crickets (*Gryllus*), the same barrier genes restricted gene flow in two sections of the hybrid zone and were linked to intrinsic factors of prezygotic isolation (Larson, Andrés, et al., 2013; Larson, Guilherme Becker, Bondra, & Harrison, 2013; Larson et al., 2014). In both these examples, the overlap of barrier genes could be linked to processes isolating the species involved.

However, more often than not, patterns of restricted introgression differ between transects in the same hybrid zone (Harrison & Larson, 2016, and references therein). In the well-studied house mouse hybrid zone (*Mus*), patterns of restricted gene flow differ among transects, suggesting several different genetic architectures of isolation between the two species (Teeter et al., 2009). However, some markers appeared to show restricted introgression in both transects in *Mus*, and were linked to hybrid sterility in laboratory settings (Janoušek et al., 2012). The presence of both similarities and differences in the barrier effect in independent transects in the *Bufo* hybrid zone thus appears to be highly comparable to the findings in the *Mus* hybrid zone.

Differences in introgression between the Bufo *transects*

A notable difference between the two transects is asymmetric introgression in transect one compared to symmetric introgression in transect two. In northwest France (transect one), Bayesian genomic clines analysis indicate significant asymmetry in directional introgression from *B. bufo* into *B. spinosus* ($\alpha < 0$ in 151 markers is significantly higher than $\alpha > 0$ in 110 markers) and a shift in the HI geographic cline based on neutral markers (Fig, 2) which shows asymmetric neutral introgression from *B. spinosus* into *B. bufo*. In southeast France (transect two), these two approaches reveal equal amounts of introgression on both sides of the hybrid zone. In northwest France, such a tail of introgression to the north was previously interpreted as a tail of introgression in the wake of (past) hybrid zone movement, and the hybrid zone was

assumed to have stabilised at a gradient of elevation (Arntzen et al., 2016). The pattern of introgression currently observed, a tail towards the north with a coincident peak of admixture linkage disequilibrium (D') is highly similar to the pattern observed in van Riemsdijk et al. (2018), and is most consistent with asymmetric reproductive isolation due to mating preferences or mitonuclear incompatibilities, but does not exclude the possibility of a moving hybrid zone. The asymmetry of introgression combined with a (slightly) displaced peak could also be the result of past hybrid zone movement, where the peak of D' has been broken down by recombination, because the increased gene flow from the *B. bufo* side of the hybrid zone has been reduced recently. In southeast France the zone appears to be stable, with a symmetric pattern of introgression, and a narrower transition than in northwest France. The differences in asymmetric and symmetric introgression between transects can be explained by either intrinsic (genetically determined) factors or extrinsic factors.

The presence of multiple genetic groups involved in the two transects would support an intrinsic cause of the differences in introgression. The *B. bufo* toads involved in the two transects show intraspecific divergence, with *B. bufo* in northwest France representing an mtDNA clade that resided in a refugium in the northern Balkans during the last glacial maximum (22,000 BP), whilst *B. bufo* in southeast France carry mtDNA variants that survived in Italy, and in the northern and western Balkans (Garcia-Porta et al., 2012; Recuero et al., 2012; Arntzen et al., 2017). Meanwhile, *B. spinosus* individuals from France belong to a lineage derived from a single Iberian refugium (Garcia-Porta et al., 2012; Recuero et al., 2012; Arntzen et al., 2017). Furthermore, previous research showed structural differences in chromosome morphology in subgroups of *B. bufo*, with homomorphic chromosomes for both sexes in Russian toads (which presumably is the same mitochondrial clade occurring in northwest France), but one heteromorphic chromosome for female toads in Italy, whereas chromosome morphology within *B. spinosus* appears to be uniform (Morescalchi, 1964;

Birstein & Mazin, 1982; Pisanets et al., 2009; Skorinov et al., 2018). Intraspecific mitochondrial and chromosome morphology differences within *B. bufo* are likely reflected by (other) nuclear genetic substructure. The Structure and PCA results, however, did not indicate the presence of multiple genetic subgroups on the *B. bufo* side of the hybrid zone, despite the inclusion of all 4,863 RAD markers obtained. The lack of a signal indicating an additional genetic subgroup within *B. bufo* may be due to the lack of (pure) parental populations in southwest France for this subgroup (Rogers & Bohlender, 2015), which we are likely to have missed with the current sampling scheme (Fig. 1). An extended phylogeographic study based on nuclear DNA could confirm the presence of the involvement of multiple *B. bufo* subgroups in the hybrid zone.

Different extrinsic factors may also influence the variation in introgression between both transects. The geography of the northwest transect is relatively homogeneous compared to the southwest transect (e.g. altitude, Fig. 1). The hybrid zone in southeast France locally runs in parallel to landscape features (rivers and mountains) that are associated with the species range border (Arntzen et al., 2018). Barrier genes may be coupled to a steep gradient of local adaptive genes between two populations and stabilise a hybrid zone at an ecotone, even if the local adaptations would also be beneficial in populations outside the hybrid zone (Bierne et al., 2011). The hybrid zone in southeast France may thus be trapped at a steep gradient of locally adaptive markers.

When studying single transects, often more than one explanation for asymmetric introgression across a hybrid zone are reported. Providing solid proof of hybrid zone movement or asymmetric reproductive isolation proves to be difficult (Buggs, 2007; Toews & Brelsford, 2012; Brandvain, Pauly, May, & Turelli, 2014; Wielstra, 2019). Yet some studies provide convincing support for one explanation over the other by combining multiple lines of evidence. For example, in a group of Neotropical jacanas (*Jacana*), females of the larger and more

aggressive species more often mother hybrid offspring in sympatric regions, which resulted in a shift of female body mass relative to the genetic cline centre (Lipshutz et al., 2019). In crested newts (*Triturus*), the occurrence of enclaves, predictions of climate models, and asymmetric introgression support hybrid zone movement as a cause of asymmetric introgression (Wielstra & Arntzen, 2012; Wielstra, Burke, Butlin, & Arntzen, 2017). For the *Bufo* hybrid zone, additional evidence in the form of behavioural, breeding, or (climate) simulation studies may thus provide stronger support for either an intrinsic or an extrinsic cause of the asymmetric introgression observed in northwest France.

Conclusion

We find an overlap of barrier markers between the two transects, which indicates that in the *Bufo* hybrid zone a range wide barrier effect has evolved. The barrier effect is strong enough to have prevented the two *Bufo* species from merging despite secondary contact being many millennia old. However, within different subgroups of *B. bufo*, reinforcement seems to be following different paths. This might not only explain the overlap of barrier markers and the difference in the barrier effect, but also the difference in the asymmetric and symmetric introgression in the two sections. In both sections, introgression of *B. bufo* genetic material into *B. spinosus* towards the south is equally restricted. In northwest France introgression is less restricted from *B. spinosus* into *B. bufo*, because reinforcement has been occurring for a shorter time. In southeast France introgression is more restricted as reinforcement within *B. bufo* has been ongoing for a longer time. Genetic substructure within one of the species involved results in a complex situation, and future research on the *Bufo* hybrid zone should focus on delineating potential intraspecific substructure in the hybrid zone based on genome-wide nuclear DNA data. The generation of a high-density linkage map or reference genome will be helpful to infer patterns of linkage and barrier loci in more detail. Laboratory crosses of individuals from the

resulting intraspecific *B. bufo* groups and *B. spinosus* could verify the modes of (asymmetric) reproductive isolation (e.g. Malone & Fontenot, 2008; Stöck et al., 2013; Brandvain et al., 2014). The *Bufo* hybrid zone provides an excellent opportunity to separate a general barrier to gene flow from idiosyncrasies in gene flow specific to individual transects.

References

Abbott, R., Albach, D., Ansell, S., Arntzen, J. W., Baird, S. J. E., Bierne, N., … Zinner, D. (2013). Hybridization and speciation. *Journal of Evolutionary Biology*, *26*, 229–246. https://doi.org/10.1111/j.1420-9101.2012.02599.x

Arntzen, J. W., de Vries, W., Canestrelli, D., & Martínez-Solano, I. (2017). Hybrid zone formation and contrasting outcomes of secondary contact over transects in common toads. *Molecular Ecology*, *26*, 5663–5675. https://doi.org/10.1111/mec.14273

Arntzen, J. W., McAtear, J., Butôt, R., & Martínez-Solano, I. (2018). A common toad hybrid zone that runs from the Atlantic to the Mediterranean. *Amphibia-Reptilia*, *39*, 41–50. https://doi.org/10.1163/15685381-00003145

Arntzen, J. W., Trujillo, T., Butot, R., Vrieling, K., Schaap, O. D., Gutiérrez-Rodriquez, J., & Martinez-Solano, I. (2016). Concordant morphological and molecular clines in a contact zone of the common and spined toad (*Bufo bufo* and *B. spinosus*) in the northwest of France. *Frontiers in Zoology*, *13*, 1–12. https://doi.org/10.1186/s12983-016-0184-7

Baird, S. J. E. (2015). Exploring linkage disequilibrium. *Molecular Ecology Resources*, *15*, 1017–1019. https://doi.org/10.1111/1755-0998.12424

Barton, N. H. (1983). Multilocus clines. *Evolution*, *37*, 454–471. https://doi.org/10.2307/2408260

Barton, N. H. (2001). The role of hybridization in evolution. *Molecular Ecology*, *10*, 551–568. https://doi.org/10.1046/j.1365-294X.2001.01216.x

Barton, N. H. (2013). Does hybridization influence speciation? *Journal of Evolutionary Biology*, *26*, 267–269. https://doi.org/10.1111/jeb.12015

Barton, N. H., & Gale, K. S. (1993). Genetic analysis of hybrid zones. In R. G. Harrison (Ed.), *Hybrid zones and the evolutionary process* (pp. 13–45). New York: Oxford University Press.

Barton, N. H., & Hewitt, G. M. (1985). Analysis of hybrid zones. *Annual Review of Ecology and Systematics*, *16*, 113–148.

Bayona-Vásquez, N. J., Glenn, T. C., Kieran, T. J., Pierson, T. W., Hoffberg, S. L., Scott, P. A., … Faircloth, B. C. (2019). Adapterama III : Quadruple-indexed , double / triple- enzyme RADseq libraries (2RAD / 3RAD). *Bioarxiv*, 1–7. https://doi.org/http://dx.doi.org/10.1101/205799

Benestan, L. M., Ferchaud, A.-L., Hohenlohe, P. A., Garner, B. A., Naylor, G. J. P., Baums, I. B., … Luikart, G. (2016). Conservation genomics of natural and managed populations: building a conceptual and practical framework. *Molecular Ecology*, *25*, 2967–77. https://doi.org/10.1111/mec.13647

Bierne, N., Welch, J., Loire, E., Bonhomme, F., & David, P. (2011). The coupling hypothesis: why genome scans may fail to map local adaptation genes. *Molecular Ecology*, *20*, 2044–2072. https://doi.org/10.1111/j.1365-294X.2011.05080.x

Birstein, V. J., & Mazin, A. L. (1982). Chromosomal polymorphism of *Bufo bufo*: karyotype and C-banding pattern of *B. b. verrucosissima*. *Genetica*, *59*, 93–98. https://doi.org/10.1007/BF00133292

Brandvain, Y., Pauly, G. B., May, M. R., & Turelli, M. (2014). Explaining Darwin's corollary to Haldane's rule: The role of mitonuclear interactions in asymmetric postzygotic isolation among toads. *Genetics*, *197*, 743–747. https://doi.org/10.1534/genetics.113.161133

Buerkle, C. A., & Rieseberg, L. H. (2001). Low intraspecific variation for genomic isolation between hybridizing sunflower species. *Evolution*, *55*, 684–691. https://doi.org/10.1554/0014-

3820(2001)055[0684:livfgi]2.0.co;2

Buggs, R. J. A. (2007). Empirical study of hybrid zone movement. *Heredity*, *99*, 301–312. https://doi.org/10.1038/sj.hdy.6800997

Butlin, R. K., & Smadja, C. M. (2018). Coupling, reinforcement, and speciation. *The American Naturalist*, *191*, 155–172. https://doi.org/10.1086/695136

Chhatre, V. E., & Emerson, K. J. (2017). StrAuto: automation and parallelization of STRUCTURE analysis. *BMC Bioinformatics*, *18*, 1–5. https://doi.org/10.1186/s12859-017-1593-0

Dagilis, A. J., Kirkpatrick, M., & Bolnick, D. I. (2019). The evolution of hybrid fitness during speciation. *PLoS Genetics*, *15*, e1008125.

Derryberry, E. P., Derryberry, G. E., Maley, J. M., & Brumfield, R. T. (2014). HZAR: hybrid zone analysis using an R software package. *Molecular Ecology Resources*, *14*, 652–663. https://doi.org/10.1111/1755-0998.12209

Devitt, T. J., Baird, S. J. E., & Moritz, C. (2011). Asymmetric reproductive isolation between terminal forms of the salamander ring species *Ensatina eschscholtzii* revealed by fine-scale genetic analysis of a hybrid zone. *BMC Evolutionary Biology*, *11*. https://doi.org/10.1186/1471-2148-11-245

Eaton, D. A. R. (2014). PyRAD: assembly of de novo RADseq loci for phylogenetic analyses. *Bioinformatics*, *30*, 1844–1849. https://doi.org/10.1093/bioinformatics/btu121

Emelianov, I., Marec, F., & Mallet, J. (2004). Genomic evidence for divergence with gene flow in host races of the larch budmoth. *Proceedings of the Royal Society B: Biological Sciences*, *271*, 97–105. https://doi.org/10.1098/rspb.2003.2574

Evanno, G., Regnaut, S., & Goudet, J. (2005). Detecting the number of clusters of individuals using the software STRUCTURE: a simulation study. *Molecular Ecology*, *14*, 2611–2620. https://doi.org/10.1111/j.1365-294X.2005.02553.x

Excoffier, L., Foll, M., & Petit, R. J. (2009). Genetic consequences of range expansions. *Annual Review of Ecology, Evolution, and Systematics*, *40*, 481–501. https://doi.org/10.1146/annurev.ecolsys.39.110707.173414

Fitzpatrick, B. M. (2012). Estimating ancestry and heterozygosity of hybrids using molecular markers. *BMC Evolutionary Biology*, *12*, 131. https://doi.org/10.1186/1471-2148-12-131

Francis, R. M. (2017). POPHELPER: an R package and web app to analyse and visualize population structure. *Molecular Ecology Resources*, *17*, 27–32. https://doi.org/10.1111/1755-0998.12509

Garcia-Porta, J., Litvinchuk, S. N., Crochet, P. A., Romano, A., Geniez, P. H., Lo-Valvo, M., … Carranza, S. (2012). Molecular phylogenetics and historical biogeography of the west-palearctic common toads (*Bufo bufo* species complex). *Molecular Phylogenetics and Evolution*, *63*, 113–130. https://doi.org/10.1016/j.ympev.2011.12.019

Gay, L., Crochet, P. A., Bell, D. A., & Lenormand, T. (2008). Comparing clines on molecular and phenotypic traits in hybrid zones: a window on tension zone models. *Evolution*, *62*, 2789–2806. https://doi.org/10.1111/j.1558-5646.2008.00491.x

Glenn, T. C., Nilsen, R. A., Kieran, T. J., Finger Jr., J. W., Pierson, T. W., Bentley, K. E., … Faircloth, B. C. (2016). Adapterama I: universal stubs and primers for thousands of dual-indexed Illumina libraries (iTru & iNext). *BioRxiv*.

Gompert, Z., & Buerkle, C. A. (2011). Bayesian estimation of genomic clines. *Molecular Ecology*, *20*, 2111–2127. https://doi.org/10.1111/j.1365-294X.2011.05074.x

Gompert, Z., & Buerkle, C. A. (2012). bgc: software for Bayesian estimation of genomic clines. *Molecular Ecology Resources*, *12*, 1168–1176. https://doi.org/10.1111/1755-0998.12009.x

Gompert, Z., Parchman, T. L., & Buerkle, C. A. (2012). Genomics of isolation in hybrids. *Philosophical Transactions of the Royal Society B: Biological Sciences*, *367*, 439–450. https://doi.org/10.1098/rstb.2011.0196

Graham, C. F., Glenn, T. C., McArthur, A. G., Boreham, D. R., Kieran, T., Lance, S., … Somers, C. M. (2015). Impacts of degraded DNA on restriction enzyme associated DNA sequencing (RADSeq). *Molecular Ecology Resources*, *15*, 1304–15. https://doi.org/10.1111/1755-0998.12404

Haldane, J. B. S. (1922). Sex ratio and unisexual sterility in hybrid animals. *Journal of Genetics*, *12*, 7–109. https://doi.org/10.1007/BF02983075

Harrison, R. G., & Larson, E. L. (2014). Hybridization, introgression, and the nature of species boundaries. *Journal of Heredity*, *105*, 795–809. https://doi.org/10.1093/jhered/esu033

585 Harrison, R. G., & Larson, E. L. (2016). Heterogeneous genome divergence, differential introgression,
586 and the origin and structure of hybrid zones. *Molecular Ecology*, *25*, 2454–2466.
587 https://doi.org/10.1111/mec.13582
588 Hemelaar, A. (1988). Age, growth and other population characteristics of *Bufo bufo* from different
589 latitudes and altitudes. *Journal of Herpetology*, *22*, 369–388.
590 Hewitt, G. M. (1975). A sex-chromosome hybrid zone in the grasshopper *Podisma pedestris*
591 (Orthoptera: Acrididae). *Heredity*, *35*, 375–387. https://doi.org/10.1038/hdy.1975.108
592 Hewitt, G. M. (1988). Hybrid zones - natural laboratories for evolutionary studies. *Trends in Ecology*
593 *and Evolution*, *3*, 158–167. https://doi.org/10.1016/0169-5347(88)90033-X
594 Hoffberg, S., Kieran, T., Catchen, J., Devault, A., Faircloth, B. C., Mauricio, R., & Glenn, T. C. (2016).
595 RADcap: sequence capture of dual-digest RADseq libraries with identifiable duplicates and
596 reduced missing data. *Molecular Ecology Resources*, *16*, 1264–1278.
597 https://doi.org/10.1111/jnc.13494
598 Janoušek, V., Wang, L., Luzynski, K., Dufková, P., Vyskočilová, M. M., Nachman, M. W., … Tucker,
599 P. K. (2012). Genome-wide architecture of reproductive isolation in a naturally occurring hybrid
600 zone between *Mus musculus musculus* and *M. m. domesticus*. *Molecular Ecology*, *21*, 3032–3047.
601 https://doi.org/10.1111/j.1365-294X.2012.05583.x
602 Jombart, T. (2008). adegenet: a R package for the multivariate analysis of genetic markers.
603 *Bioinformatics*, *24*, 1403–1405. https://doi.org/10.1093/bioinformatics/btn129
604 Jombart, T., & Ahmed, I. (2011). adegenet 1.3-1: new tools for the analysis of genome-wide SNP data.
605 *Bioinformatics*, *27*, 3070–3071. https://doi.org/10.1093/bioinformatics/btr521
606 Kopelman, N. M., Mayzel, J., Jakobsson, M., Rosenberg, N. A., & Mayrose, I. (2015). Clumpak: a
607 program for identifying clustering modes and packaging population structure inferences across K.
608 *Molecular Ecology Resources*, *15*, 1179–1191. https://doi.org/10.1111/1755-0998.12387
609 Larson, E. L., Andrés, J. A., Bogdanowicz, S. M., & Harrison, R. G. (2013). Differential introgression
610 in a mosaic hybrid zone reveals candidate barrier genes. *Evolution*, *67*, 3653–3661.
611 https://doi.org/10.1111/evo.12205
612 Larson, E. L., Guilherme Becker, C., Bondra, E. R., & Harrison, R. G. (2013). Structure of a mosaic
613 hybrid zone between the field crickets *Gryllus firmus* and *G. pennsylvanicus*. *Ecology and*
614 *Evolution*, *3*, 985–1002. https://doi.org/10.1002/ece3.514
615 Larson, E. L., White, T. A., Ross, C. L., & Harrison, R. G. (2014). Gene flow and the maintenance of
616 species boundaries. *Molecular Ecology*, *23*, 1668–1678. https://doi.org/10.1111/mec.12601
617 Lipshutz, S. E., Meier, J. I., Derryberry, G. E., Miller, M. J., Seehausen, O., & Derryberry, E. P. (2019).
618 Differential introgression of a female competitive trait in a hybrid zone between sex-role reversed
619 species. *Evolution*, *73*, 188–201. https://doi.org/10.1111/evo.13675
620 Macholán, M., Munclinger, P., Šugerková, M., Dufková, P., Bímová, B., Božíková, E., … Piálek, J.
621 (2007). Genetic analysis of autosomal and X-linked markers across a mouse hybrid zone.
622 *Evolution*, *61*, 746–771. https://doi.org/10.1111/j.1558-5646.2007.00065.x
623 Malone, J. H., & Fontenot, B. E. (2008). Patterns of reproductive isolation in toads. *PLoS ONE*, *3*.
624 https://doi.org/10.1371/journal.pone.0003900
625 Martin, M. (2011). Cutadapt removes adapter sequences from high-throughput sequencing reads.
626 *EMBnet.Journal*, *17*, 10. https://doi.org/10.14806/ej.17.1.200
627 Morescalchi, A. (1964). Il corredo cromosomico dei Bufonidi Italiani. *Bolletino Di Zoologia*, *31*, 827–
628 836. https://doi.org/10.1080/11250006409441116
629 Narum, S. R. (2006). Beyond Bonferroni: less conservative analyses for conservation genetics.
630 *Conservation Genetics*, *7*, 783–787. https://doi.org/10.1007/s10592-005-9056-y
631 Noor, M., Grams, K. L., Bertucci, L. A., & Reiland, J. (2001). Chromosomal inversions and the
632 reproductive isolation of species. *Proceedings of the National Academy of Sciences*, *21*, 12084–
633 12088. https://doi.org/10.1073/pnas.81.1.282
634 Nosil, P., Funk, D. J., & Ortiz-Barrientos, D. (2009). Divergent selection and heterogeneous genomic
635 divergence. *Molecular Ecology*, *18*, 375–402. https://doi.org/10.1111/j.1365-294X.2008.03946.x
636 Parchman, T. L., Gompert, Z., Braun, M. J., Brumfield, R. T., McDonald, D. B., Uy, J. A. C., …
637 Buerkle, C. A. (2013). The genomic consequences of adaptive divergence and reproductive
638 isolation between species of manakins. *Molecular Ecology*, *22*, 3304–3317.
639 https://doi.org/10.1111/mec.12201

Pisanets, E. M., Litvinchuk, S. N., Rosanov, J. M., Reminniy, V. Y., Pasynkova, R. A., & Suryadnaya, N. N. M. A. S. (2009). Common toads (Amphibia, Bufonidae, *Bufo bufo* complex) from the Ciscaucasia and north of the Caucasus: the new analysis of the problem. *Zbirnik Prats' Zool. Mus.*, *40*, 83–125.

Polechová, J., & Barton, N. (2011). Genetic drift widens the expected cline but narrows the expected cline width. *Genetics*, *189*, 227–235. https://doi.org/10.1534/genetics.111.129817

Pritchard, J. K., Stephens, M., & Donnelly, P. (2000). Inference of population structure using multilocus genotype data. *Genetics*, *155*, 945–959. https://doi.org/10.1111/j.1471-8286.2007.01758.x

Rafajlović, M., Emanuelsson, A., Johannesson, K., Butlin, R. K., & Mehlig, B. (2016). A universal mechanism generating clusters of differentiated loci during divergence-with-migration. *Evolution; International Journal of Organic Evolution*, *70*, 1609–1621. https://doi.org/10.1111/evo.12957

Ravinet, M., Faria, R., Butlin, R. K., Galindo, J., Bierne, N., Rafajlović, M., … Westram, A. M. (2017). Interpreting the genomic landscape of speciation: finding barriers to gene flow. *Journal of Evolutionary Biology*, *30*, 1450–1477. https://doi.org/10.1111/jeb.13047

Recuero, E., Canestrelli, D., Vörös, J., Szabó, K., Poyarkov, N. A., Arntzen, J. W., … Martínez-Solano, I. (2012). Multilocus species tree analyses resolve the radiation of the widespread *Bufo bufo* species group (Anura, Bufonidae). *Molecular Phylogenetics and Evolution*, *62*, 71–86. https://doi.org/10.1016/j.ympev.2011.09.008

Rice, W. R. (1989). Analyzing tables of statistical tests. *Evolution*, *43*, 223–225.

Rieseberg, L. H. (2001). Chromosomal rearrangements and speciation. *TRENDS in Ecology & Evolution*, *16*, 351–358. https://doi.org/10.1016/B978-0-12-800049-6.00074-3

Rieseberg, L. H., Whitton, J., & Gardner, K. (1999). Hybrid zones and the genetic architecture of a barrier to gene flow between two sunflower species. *Genetics*, *152*, 713–727.

Rogers, A. R., & Bohlender, R. J. (2015). Bias in estimators of archaic admixture. *Theoretical Population Biology*, *100*, 63–78. https://doi.org/10.1016/j.tpb.2014.12.006

Rousset, F. (2008). GENEPOP'007: a complete re-implementation of the GENEPOP software for Windows and Linux. *Molecular Ecology Resources*, *8*, 103–106. https://doi.org/10.1111/j.1471-8286.2007.01931.x

Schumer, M., Xu, C., Powell, D. L., Durvasula, A., Skov, L., Holland, C., … Przeworski, M. (2018). Natural selection interacts with recombination to shape the evolution of hybrid genomes. *Science*, *660*, 656–660. https://doi.org/10.1126/science.aar3684.Natural

Skorinov, D. V, Bolshakova, D. S., Donaire, D., Pasynkova, R. A., Litvinchuk, S. N., & Litvinchuk, B. (2018). Karyotypic analysis of the spined toad, *Bufo spinosus* Daudin, 1803 (Aphibia: Bufonidae). *Russian Journal of Herpetology*, *25*, 253–258. https://doi.org/10.30906/1026-2296-2018-25-4-253-258

Stöck, M., Savary, R., Betto-Colliard, C., Biollay, S., Jourdan-Pineau, H., & Perrin, N. (2013). Low rates of X-Y recombination, not turnovers, account for homomorphic sex chromosomes in several diploid species of Palearctic green toads (*Bufo viridis* subgroup). *Journal of Evolutionary Biology*, *26*, 674–682. https://doi.org/10.1111/jeb.12086

Teeter, K., Thibodeau, L. M., Gompert, Z., Buerkle, C. A., C.Nachman, M. W., & Tucker, P. K. (2009). The variable genomic architecture of isolation between hybridizing species of house mice. *Evolution*, *64*, 472–485. https://doi.org/10.1111/j.1558-5646.2009.00846.x

Toews, D. P. L., & Brelsford, A. (2012). The biogeography of mitochondrial and nuclear discordance in animals. *Molecular Ecology*, *21*, 3907–3930. https://doi.org/10.1111/j.1365-294X.2012.05664.x

van Riemsdijk, I., Butlin, R. K., Wielstra, B., & Arntzen, J. W. (2018). Testing an hypothesis of hybrid zone movement for toads in France. *Molecular Ecology*, *28*, 1070–1083. https://doi.org/10.1111/mec.15005

Vines, T. H., Dalziel, A. C., Albert, A. Y. K., Veen, T., Schulte, P. M., & Schluter, D. (2016). Cline coupling and uncoupling in a stickleback hybrid zone. *Evolution*, *70*, 1023–1038. https://doi.org/10.1111/evo.12917

Wang, L., Luzynski, K., Pool, J. E., Janoušek, V., Dufkovú, P., Vyskočilovú, M. M., … Tucker, P. K. (2011). Measures of linkage disequilibrium among neighbouring SNPs indicate asymmetries across the house mouse hybrid zone. *Molecular Ecology*, *20*, 2985–3000.

https://doi.org/10.1111/j.1365-294X.2011.05148.x

Wickbom, T. (1945). Cytological studies on Dipnoi, Urodela, Anura, and Emys. *Hereditas*, *31*, 241–346. https://doi.org/10.1111/j.1601-5223.1945.tb02756.x

Wielstra, B. (2019). Historical hybrid zone movement: more pervasive than appreciated. *Journal of Biogeography*, 1–6. https://doi.org/10.1111/jbi.13600

Wielstra, B., & Arntzen, J. W. (2012). Postglacial species displacement in Triturus newts deduced from asymmetrically introgressed mitochondrial DNA and ecological niche models. *BMC Evolutionary Biology*, *12*, 1–12.

Wielstra, B., Burke, T., Butlin, R. K., & Arntzen, J. W. (2017). A signature of dynamic biogeography: enclaves indicate past species replacement. *Proceedings of the Royal Society Biological Sciences*, *284*, 1–6.

Wielstra, B., Burke, T., Butlin, R. K., Avcı, A., Üzüm, N., Bozkurt, E., … Arntzen, J. W. (2017). A genomic footprint of hybrid zone movement in crested newts. *Evolution Letters*, *1*, 93–101. https://doi.org/10.1002/evl3.9

Yeaman, S., & Whitlock, M. C. (2011). The genetic architecture of adaptation under migration-selection balance. *Evolution*, *65*, 1897–1911. https://doi.org/10.1111/j.1558-5646.2011.01269.x

Tables and figures

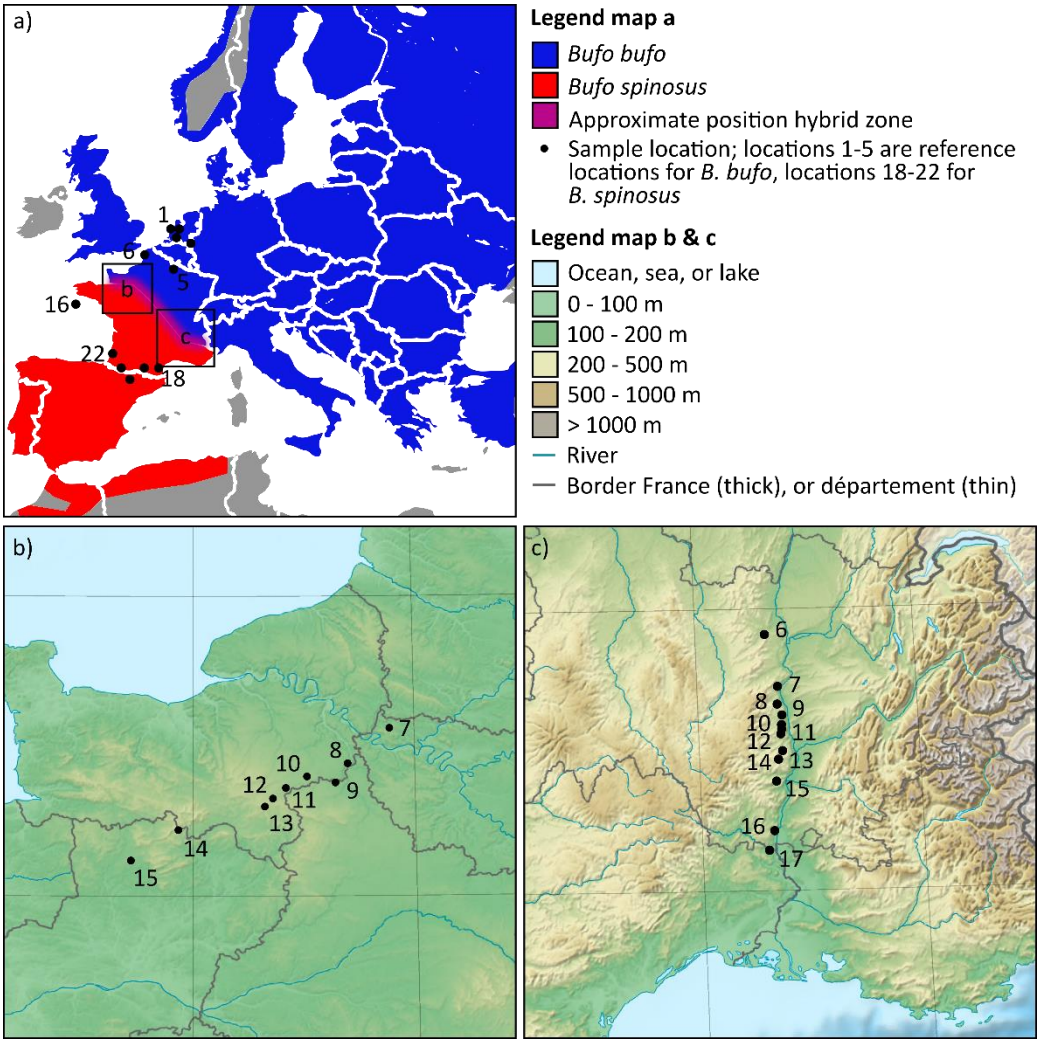

Figure 1: Overview map with a) the distribution of *Bufo bufo* and *B. spinosus*, with small squares indicating the locations of map b) for transect one in northwest France (sample locations 6-16), and map c) for transect two in southeast France (sample locations 6-17). The base map for panel b and c was downloaded from https://www.mapsland.com

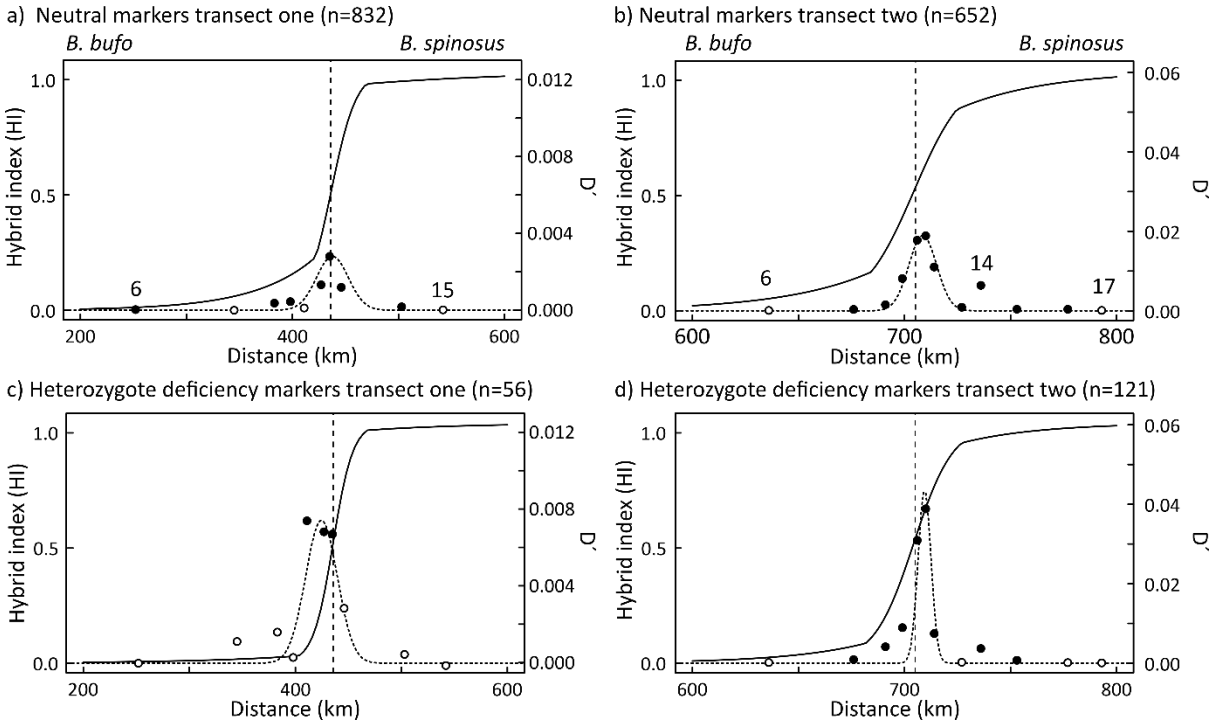

Figure 2: Geographic clines for the hybrid index (HI) and admixture linkage disequilbirium peaks (D') for neutral markers (i.e. not assigned by BGC as an outlier in any category) according to the genomic clines analysis for (a) transect one and (b) transect two, and for heterozygote deficiency markers ($\beta > 0$) for (c) transect one and (d) for transect two. The x-axis shows distance along the transect. The y-axis on the left shows the HI (solid line), and the y-axis on the right shows D' (dotted line and dots). Note that for transect one, the x-axis is twice as long as for transect two, and the right y-axis for transect one is five times shorter than for transect two. Solid dots show D' significantly different from zero, whilst open dots are not significantly different from zero, based on 95% confidence intervals.

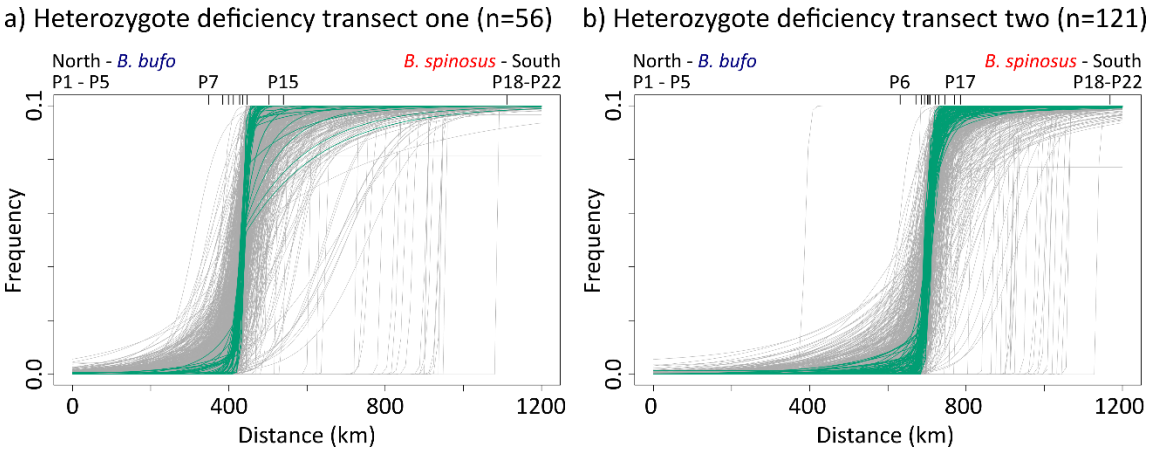

Figure 3: Geographic clines for markers showing barrier markers (green) for (a) transect one and (b) transect two with frequency of the *B. spinosus* allele on the y-axis and distance along the transect on the x-axis. Inward ticks on the top of the graph and notation near inward ticks on the top of the graph (P) refers to locations in Fig. 1.

Table 1: Bayesian genomic cline (BGC) results comparing significant outliers for transect one (T1) and transect two (T2), and the markers which were outliers in both transects (overlap), where significance of outliers is based on the exclusion of 0 in the 99.9% confidence interval (CI). The total number of markers analysed was 1,189.

Outlier	Biological interpretation	T1	T2	Overlap
$\alpha < 0$	Directional introgression from *B. bufo* into *B. spinosus*	151†	185‡	92§
$\alpha > 0$	Directional introgression from *B. spinosus* into *B. bufo*	110†	174‡	49§
$\beta < 0$	Heterozygote excess	50	105	11¶
$\beta > 0$	Heterozygote deficiency	56	123	26§

The significance tests are; (1) a Chi-squared comparing the values α outliers of only T1 and T2 to see if there is a significant difference in the number of outliers between the transects. A 2x2 contingency Chi-squared (2) was done to see if the overlap between the transects of both α and β outliers could be a coincidence, or is unlikely to have occurred under a model of random resampling.

†Significant Chi-squared with 6.4406, df = 1, P = 0.0112

‡Not significant Chi-squared with 0.3371, df = 1, P = 0.5615

§Significant 2x2 contingency Chi-squared with 285.05, 91.629, 81.288, df = 1, $P < 2.2e^{-16}$

¶Significant 2x2 contingency Chi-squared with 10.331, df = 1, P = 0.001308